# THE RELATIONSHIP OF POST-STIMULUS TIME AND INTERVAL HISTOGRAMS TO THE TIMING CHARACTERISTICS OF SPIKE TRAINS

DON H. JOHNSON, *Research Laboratory of Electronics, Massachusetts Institute of Technology, Cambridge, Massachusetts 02139, and Eaton-Peabody Laboratory of Auditory Physiology, Massachusetts Eye and Ear Infirmary, Boston, Massachusetts 02114 U.S.A.*

ABSTRACT PST (post-stimulus time) and interval histograms computed from recorded spike trains are related to an average timing characteristics of the spike train. The exact nature of this relationship varies with recording parameters, interfering signals, the histogram bin width, and the duration of the measurement interval. This work describes the conditions under which a PST histogram can serve as an unbiased estimate of the ensemble average of a spike train's intensity and an interval histogram can serve as an unbiased estimate of the probability density function of the interspike intervals. Simulation studies are used to confirm the validity of the theoretical results. As an example of an application, these results are used to analyze recordings of single-unit activity in the eighth cranial nerve.

## INTRODUCTION

Single neurons transmit information over long distances in the nervous system by means of sequences of action potentials (spike trains). In many instances these spikes have nearly identical wave forms; consequently, the times of occurrence of spikes carry the neural information.

A description of a spike train well suited for the analysis of the timing of spikes is the point process model (Cox, 1962; Cox and Lewis, 1966; Perkel et al., 1967). This model can be used to describe both stochastic (e.g., irregular) and deterministic (e.g., periodic) spike trains. In this model, the occurrence of each spike corresponds to the time of an "event"; point processes are defined by describing how the probability of an event occurring varies with time. Hence, a quantitative description of the timing of spikes recorded from a neuron involves the estimation of functions related to this probability. Two types of measurements have proved especially useful and are widely used in neurophysiology: the post-stimulus-time (PST) histogram and the histogram of the interspike time intervals (interval histogram). This paper describes how these measurements are related to estimates of the underlying functions comprising a point

---

Dr. Johnson's present address is: Department of Electrical Engineering, Rice University, Houston, Texas 77001.

process description of a spike train. Furthermore, this work contains an analysis of how these estimates are affected by recording parameters, interfering signals in the recording, and histogram parameters.

## METHODS

This paper is concerned primarily with theoretical aspects of the computation of histograms from recorded spike trains. Empirical confirmation of certain theoretical results was obtained by creating simulated spike trains with identical spike wave forms and known statistics. Each simulated spike was obtained from a Tektronix 162 waveform generator (Tektronix, Inc., Beaverton, Ore.) (wave form shown in Fig. 3).

A simulated spike train having statistics independent of time was obtained by triggering the wave form generator with a noise generator. Spike trains having statistics that varied sinusoidally in time were obtained by triggering on the sum of random noise and a sine wave.

In some tests, signals were added to the simulated spike train to emulate periodic (Fig. 3) or random (Fig. 7) interfering signals. Periodic interfering signals were obtained from a Wavetek 157 oscillator (Wavetek, San Diego, Calif); random interfering signals were obtained from a General Radio 1381 noise generator set to a bandwidth of 5 kHz (GenRad, Concord, Mass.).

## ESTIMATION OF THE INTENSITY OF A SPIKE TRAIN: THE PST HISTOGRAM

A spike train can be described mathematically as a regular stochastic point process (Snyder, 1975). A stochastic point process consists of a series of events—spikes in this case—which occur at random instants of time. This description presumes that the important aspect of a spike train is the time of occurrence of each spike; details of the spike wave form are ignored. The timing of events in a point process is influenced by $\mu(t, N(t), \mathbf{w})$, the intensity or instantaneous rate of the point process. $N(t)$ denotes the number of events occurring before time $t$ and the vector $\mathbf{w}$ denotes the times of occurrence of the previous $N(t)$ events $w_1, \ldots, w_{N(t)}$. The intensity of a regular point process determines the conditional probability of an event occurring during any small time interval.

$$\text{Prob}\,[N(t + \Delta t) - N(t) = 1 \mid N(t), \mathbf{w}] = \mu(t, N(t), \mathbf{w})\Delta t, \tag{1a}$$

$$\text{Prob}\,[N(t + \Delta t) - N(t) > 1 \mid N(t), \mathbf{w}] = 0\,(t, \Delta t). \tag{1b}$$

$N(t + \Delta t) - N(t)$ equals the number of events occurring in the interval $[t, t + \Delta t)$ and $\lim_{\Delta t \to 0} 0(t, \Delta t)/\Delta t = 0$. Eq. 1*b* defines a regular point process; no more than one event can occur at any given time.

The intensity of a spike train is a function not only of an independent time function (e.g., a stimulus) but also of the history of the point process (Eq. 1*a*). This history is expressed by the number of events occurring before time $t$ ($N(t)$) and by the times at which these events occurred ($w_1, \ldots, w_{N(t)}$). For instance, the probability of a spike occurring at a particular instant of time may depend on when previous spikes occurred (e.g., the refractory property of neuronal discharges). By averaging over all possible histories of a point process, the overall effect of previous events on the present can be

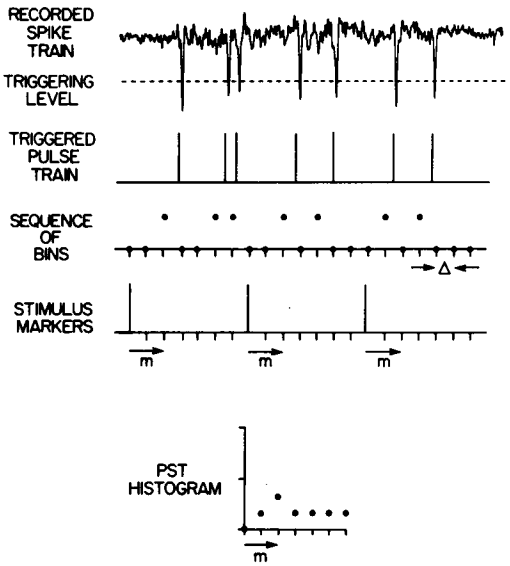


FIGURE 1 Steps in the computation of a PST histogram, illustrated for a segment of a spike recording. The explanation is given in the text.

assessed. As a consequence of this averaging, the unconditional probability of an event occurring in $[t, t + \Delta t)$ is given by:

$$\text{Prob}\,[N(t + \Delta t) - N(t) = 1] = \lambda(t)\Delta t, \tag{2}$$

where $\lambda(t)$ denotes the average of the intensity $\mu(t, N(t), \mathbf{w})$ over all possible realizations of the point process before time $t$.

A PST histogram is computed from a recorded train of spike discharges in three steps (Fig. 1).

MEASUREMENT OF TIME OF OCCURRENCE OF EACH SPIKE The recorded spike train serves as the input to a triggered pulse generator; the resulting output pulse train denotes the time at which the recorded spike train crosses a specified level with a specific slope polarity. With an appropriately chosen trigger level, each output pulse corresponds to a spike.

TIME QUANTIZATION The time axis of the triggered pulse train is quantized into equal intervals (bins). The number of spikes occurring in each bin is measured. By this process, a sequence is defined with each element of the sequence corresponding to a bin and having a value equal to the number of spikes in the bin.

SYNCHRONIZATION AND AVERAGING A PST histogram is computed from this sequence by adding together the contents of bins which occur at a specific time relative to a series of stimulus markers.

The following analysis demonstrates that the PST histogram is an estimate of the average intensity $\lambda(t)$. Furthermore, the accuracy of this estimate is affected by interfering signals, finite bin widths, and the duration of the data.

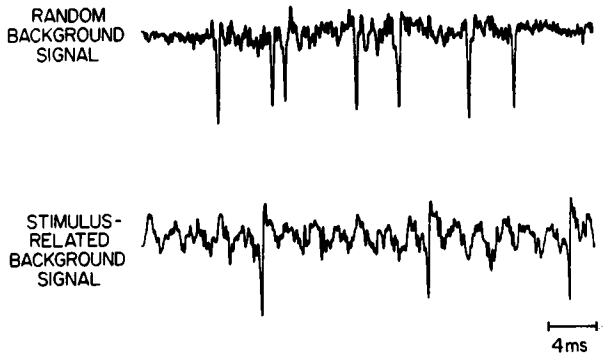


FIGURE 2 Waveforms of recorded neuronal spike trains. Two examples are shown. Each recording was obtained with platinum-indium microelectrodes (Gesteland et al., 1959) from a single neuron in the cochlear nucleus of the cat. The upper trace demonstrates the occurrence of random background noise in spike train recordings. The lower trace was obtained from a unit responding to a 500-Hz tone. A background interfering signal having the same period as the stimulus is evident in the recording.

### *The Effect of Interfering Signals on Spike Triggering*

Spikes are always recorded in the presence of background electrical interference (Fig. 2). This interference may be a random fluctuation of the recorded potential unrelated to the spike activity; for example, noise interference can result from electrical processes in the electrode or in the tissue. In addition, the interference may contain a deterministic component related to a physical stimulus (Fig. 2). Such signals can be of physiological origin, e.g., the response of large populations of cells to a stimulus. The presence of an interfering background signal, whether stochastic or deterministic, limits the accuracy of measuring the time of occurrence of a spike and reduces the accuracy of estimating $\lambda(t)$ from such data. An analysis of such errors follows.[1]

The most common method used to estimate the time of occurrence of a spike is the triggering method (Glaser and Ruchkin, 1976). Let $s(t)$ denote a spike train without interfering signals. A pulse is triggered at the moment $t_0$ when a spike crosses the threshold level $v_T$ in the proper direction (Fig. 1). For a negative-going spike, this trigger time is defined by:[2]

$$s(t_0) = v_T; \left.\frac{ds}{dt}\right|_{t=t_0} < 0. \tag{3}$$

This time, $t_0$, defines the time of occurrence of the spike in the triggering method. Now assume that the recorded signal consists of a spike train $s(t)$ and an additive in-

[1]The following derivation, culminating in Eq. 9, is drawn from an unpublished memorandum: E. C. Moxon. 1971. Effect of a spurious additive signal on apparent time-of-occurrence of finite-rise-time pulses as determined from level crossings.

[2]In the following, the negative-going threshold crossing is chosen to illustrate the theory. In practice, the sign of the spike's slope at the trigger point can be either positive or negative without affecting the result.

terfering signal $i(t)$. A pulse is triggered from this signal at the time $\tilde{t}_0$ when the recorded signal crosses the threshold $v_T$ in the proper direction.

$$s(\tilde{t}_0) + i(\tilde{t}_0) = v_T; \left.\frac{d(s + i)}{dt}\right|_{t=\tilde{t}_0} < 0. \tag{4}$$

In order to relate $\tilde{t}_0$ to $t_0$, approximate $s(\tilde{t}_0)$ by a truncated Taylor series expansion:

$$s(\tilde{t}_0) = s(t_0) + m_s(\tilde{t}_0 - t_0), \tag{5}$$

where $m_s$ denotes the derivative of $s(t)$ at $t_0$. This approximation is valid only if the time difference $(\tilde{t}_0 - t_0)$ is small. This presumption implies that the interfering signal $i(t)$ is relatively small in amplitude so that the probability of false triggers (triggering on the interfering signal instead of on a spike), missed triggers (completely missing the presence of a spike), or multiple triggers (triggering two or more pulses from one spike) is small. The trigger time $\tilde{t}_0$ is related to $t_0$, the time of occurrence of the spike, by:

$$\tilde{t}_0 = t_0 - i(\tilde{t}_0)/m_s. \tag{6}$$

The term $i(\tilde{t}_0)/m_s$ represents a jitter in the trigger time $\tilde{t}_0$ about the true time $t_0$.

Because every triggered pulse corresponds to a spike, the probability of a spike occurring in the interval $[t, t + \Delta t)$ must be equal to the probability of a triggered pulse occurring in $[\tilde{t}, \tilde{t} + \Delta\tilde{t})$. Defining $\tilde{\lambda}(t)$ to be the average of the intensity of the triggered pulse train, this condition is expressed by:

$$\tilde{\lambda}(\tilde{t})\Delta\tilde{t} = \lambda(t)\Delta t. \tag{7}$$

In the limit of small $\Delta t$, $\tilde{\lambda}(t)$ is related to $\lambda(t)$ by:

$$\tilde{\lambda}(\tilde{t}) = (dt/d\tilde{t})\,\lambda(t). \tag{8}$$

Using Eq. 6, this expression is written:

$$\tilde{\lambda}(t) = [1 + i'(t)/m_s]\,\lambda(t + i(t)/m_s), \tag{9}$$

where $i'(t)$ denotes the derivative of the interfering signal $i(t)$. Consequently, $\tilde{\lambda}(t)$ depends not only upon the average $\lambda(t)$ of the intensity of the recorded spike train, but also upon the characteristics of $i(t)$. The disparity between $\tilde{\lambda}(t)$ and $\lambda(t)$ is manifested in two ways: an amplitude modulation by the factor $[1 + i'(t)/m_s]$ which depends upon the derivative of the interfering signal and a time jitter of amplitude $i(t)/m_s$ in the time dependence of $\lambda(t)$.

The effect of the amplitude modulation term is demonstrated when $\lambda(t)$ is a constant $(\lambda_0)$. In this case, although the average intensity of the spike train is independent of time, the intensity of the triggered pulse train can show an artifactual time dependence:

$$\tilde{\lambda}(t) = [1 + i'(t)/m_s] \cdot \lambda_0. \tag{10}$$

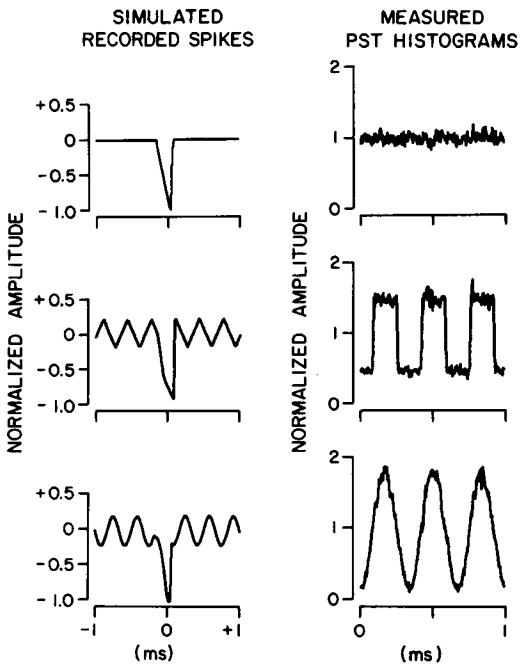


FIGURE 3 Effect of periodic interfering signals on measured PST histograms. Individual simulated spikes with additive periodic interfering signals are shown in the left column. Each simulated spike is a negative pulse whose falling phase is linear with a duration of 200 $\mu$s. The PST histograms computed from these spike trains are shown in the right column. Each of these histograms was synchronized to every third positive-going zero-crossing of the interfering signal. The simulated spikes occurred at random with respect to the interfering signal. The vertical scale of each histogram was normalized so that its average value corresponds to unity. The bin width of each histogram was 5 $\mu$s and approximately 63,000 spikes were used to compute each histogram. The simulated spike train with no interfering signal had a constant intensity (top row). When a triangle-wave interfering signal (peak value of 0.2 relative to the amplitude of the spike and frequency of 3 kHz) was added to this spike train, the resulting histogram resembled a square wave (middle row). Eq. 10 predicts that such an interfering signal would produce a square wave having peak-to-peak amplitude 0.96 in the histogram; the measured peak-to-peak value is 1.02. A sinusoidal interfering signal (peak value of 0.2 relative to the amplitude of the spike and frequency of 3 kHz) produced a cosinusoidal wave form in the measured PST histogram (bottom row). The theory predicts such a wave form with a peak-to-peak amplitude of 1.51; the measured peak-to-peak value is 1.61.

To test the validity of Eq. 10, various interfering signals were added to a simulated spike train having a constant average intensity and then $\tilde{\lambda}(t)$ was estimated. According to Eq. 10, if $i(t)$ were a triangle wave, the intensity $\tilde{\lambda}(t)$ should be a square wave. Results of the simulation for this case (Fig. 3) are accurately predicted by Eq. 10. In a second simulation, the interfering signal was a sinusoid. Such a background signal can occur, for example, when recordings are obtained from neural units while sinusoidal stimuli are being used (Fig. 2). This type of interfering signal can result from the recording of sinusoidal extracellular potentials or, if care is not taken, from electrical cross talk between the stimulus generator and the recording electrode. Letting $i(t)$ =

$A \sin(2\pi ft)$, Eq. 10 is written:

$$\tilde{\lambda}(t) = [1 + (2\pi fA/m_s) \cos 2\pi ft] \cdot \lambda_0. \tag{11}$$

Approximate $m_s$, the slope of the spike at the trigger point, by:

$$m_s = \text{peak}[s(t)]/t_r, \tag{12}$$

where $t_r$ is the rise-time of the spike measured from the initial portion of the spike to its peak and peak $[s(t)]$ is the peak amplitude of the spike. Eq. 12 is satisfied exactly for the simulated spikes shown in Fig. 3. By defining $\gamma$ to be the ratio of the rms amplitude of the interfering signal to the peak amplitude of the spike, $\gamma = (A/\sqrt{2})/\text{peak}[s(t)]$, Eq. 11 can be written:

$$\tilde{\lambda}(t) = [1 + \sqrt{8}\pi\gamma t_r \cos 2\pi ft] \cdot \lambda_0. \tag{13}$$

Consequently, $\tilde{\lambda}(t)$ is cosinusoidal (Fig. 3). Simulation studies show (Fig. 4) that the amplitude of this time-varying artifact is accurately predicted by Eq. 13. This amplitude is proportional to the product of the frequency $f$, the noise-to-signal ratio $\gamma$, and the rise-time of the spike $t_r$.

The effect of the time-jitter term in Eq. 9 is illustrated by assuming that $\lambda(t)$ is sinusoidal,

$$\lambda(t) = \bar{\lambda} \cdot [1 + 2S_f \cos 2\pi ft], \tag{14}$$

and that the interfering signal is a stationary stochastic process having a Gaussian amplitude density, zero mean, variance $\sigma^2$, and autocorrelation function $R_i(\tau)$.

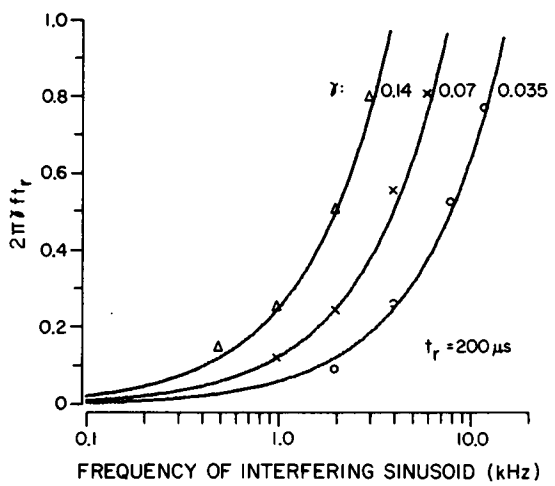


FIGURE 4 The predicted amplitude of sinusoidal response induced in the intensity of a spike train by a sinusoidal interfering signal (Eq. 13) is shown by the solid curves for three values of $\gamma$. The computation of these curves presumed that the spike rise time $t_r$ for the spike was 200 $\mu$s. Measurements of the amplitude of the induced sinusoidal component in the resulting PST histogram were made for these values of $\gamma$: $\Delta$, $\gamma = 0.14$; $\times$, $\gamma = 0.07$; $\circ$, $\gamma = 0.035$.

Such a recording situation could represent a spike train synchronized to a sinusoidal sensory stimulus (Kiang et al., 1965; Rose et al., 1967) recorded in the presence of additive random interfering noise. Using Eq. 9, the average intensity of a pulse train triggered from such a recording is given by:

$$\tilde{\lambda}(t) = \bar{\lambda} \cdot [1 + 2S_f \cos 2\pi f(t + i(t)/m_s)] \cdot [1 + i'(t)/m_s]. \tag{15}$$

Consequently, the expected value of $\tilde{\lambda}(t)$, $E[\tilde{\lambda}(t)]$, the degree to which frequency information in $\lambda(t)$ is reflected in the average properties of $\tilde{\lambda}(t)$ can be determined. With certain restrictions on $R_i(\tau)$, $E[\tilde{\lambda}(t)]$ does not depend upon the modulation term $i'(t)/m_s$ (see the Appendix) and is given by:

$$E[\tilde{\lambda}(t)] = \bar{\lambda} \cdot [1 + 2S_f H_i(f) \cos 2\pi ft], \tag{16}$$

where:

$$H_i(f) = \exp\{-\tfrac{1}{2}(2\pi f\sigma/m_s)^2\}. \tag{17}$$

Writing Eq. 17 in terms of the noise-to-signal ratio $\gamma$ ($\gamma = \sigma/\text{peak}\,[s(t)]$) yields:

$$H_i(f) = \exp\{-\tfrac{1}{2}(2\pi f\gamma t_r)^2\}. \tag{18}$$

The result given in Eq. 16 can be generalized. If $\lambda(t)$ can be described as a finite sum of sinusoidal components of frequency $f_k$

$$\lambda(t) = \bar{\lambda} \cdot [1 + 2\Sigma S_{f_k} \cos 2\pi f_k t], \tag{19}$$

then $E[\tilde{\lambda}(t)]$ contains each of these components but reduced in amplitude by the factor $H_i(f_k)$.

$$E[\tilde{\lambda}(t)] = \bar{\lambda} \cdot [1 + 2\Sigma S_{f_k} H_i(f_k) \cos 2\pi f_k t]. \tag{20}$$

Therefore, the average effects of a random interfering signal on measurements of $\lambda(t)$ can be described as passing $\lambda(t)$ through a linear, time-invariant, low pass filter having frequency response $H_i(f)$. Letting $\tilde{\Lambda}(f)$ and $\Lambda(f)$ denote the Fourier transforms of $E[\tilde{\lambda}(t)]$ and $\lambda(t)$ respectively, this result is expressed as:

$$\tilde{\Lambda}(f) = H_i(f) \cdot \Lambda(f). \tag{21}$$

The frequency response of the filter $H_i(f)$ is shown in Fig. 5, together with results obtained from a simulation. The theoretical and experimental results agree sufficiently well to establish the general validity of Eq. 21. The bandwidth $f_B$ of the filter $H_i(f)$ can be defined as the frequency at which $H_i(f) = \exp(-0.5)$. This bandwidth is given by:

$$f_B = (2\pi\gamma t_r)^{-1}. \tag{22}$$

Frequency components in $\lambda(t)$ that are much less than $f_B$ are unaffected by random interfering signals; components comparable to or larger than $f_B$ are attenuated.

In summary, interfering signals that corrupt the recording of a spike train can affect

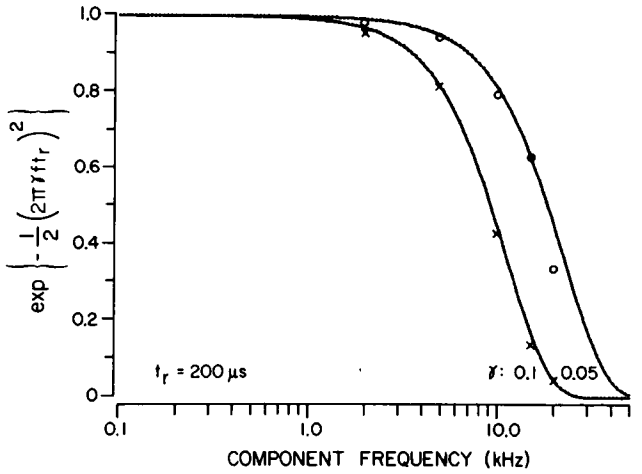


FIGURE 5 Reduction of the sinusoidal component in a measured intensity due to additive noise in the recording. The intensity of a spike train is assumed to contain a sinusoidal component (Eq. 14) and the recording corrupted by additive Gaussian noise. The predicted reduction of this sinusoidal component in the intensity $\tilde{\lambda}(t)$ by the additive noise (Eq. 16) is shown by the solid curves for two values of the noise-to-spike amplitude ratio $\gamma$. The spike rise time for the individual spikes was presumed to be 200 μs. Measurements of the sinusoidal components in PST histograms computed from these spike trains were made under two conditions: first without the presence of any interfering signal, then with Gaussian noise added to the simulated spike train. The ratio of these amplitude measurements are shown for the two values of $\lambda$: ×, $\gamma = 0.1$; ○, $\gamma = 0.05$.

measurements of the timing information in the spike train. Two kinds of effects can occur: (*a*) a deterministic interfering signal can induce an artifactual component in the measured intensity, and (*b*) a random interfering signal can act as a filter on the average of the intensity of the spike train. These effects become more severe as the amplitude of the interfering signal increases relative to the individual spikes and as the stimulus frequency is increased.

*Time-Axis Quantization*

The next step in the computation of a PST histogram is to quantize the time axis into bins of duration $\Delta$ and to specify those bins in which triggered pulses occur. The exact time of occurrence of the pulse within a bin is lost in this process. Hence, time-quantization leads to errors in representing the time of occurrence of triggered pulses.

The time-quantization process is described by defining each element of the sequence $\{x_m\}$ to be equal to the number of spikes occurring in the $m^{\text{th}}$ bin—the time interval $[m\Delta, (m + 1)\Delta)$. The expected value of $x_m$ easily shown to be:

$$E[x_m] = \int_{m\Delta}^{(m+1)\Delta} \tilde{\lambda}(\alpha)\mathrm{d}\alpha, \tag{23}$$

or more conveniently expressed as:

$$E[x_m] = \tilde{\lambda}(t) \otimes h_\Delta(t) \,|_{t=(m+1)\Delta} \tag{24}$$

where $\otimes$ denotes convolution and $h_\Delta(t)$ is the impulse response of a finite-time integrator: a linear, time-invariant filter which integrates its input signal over a specified interval of time.

$$h_\Delta(t) = \begin{cases} 1 & 0 \leq t < \Delta \\ 0 & \text{otherwise.} \end{cases} \tag{25}$$

The computation of $E[x_m]$ from $\tilde{\lambda}(t)$ can therefore be viewed as a cascade of two transformations.

First, the intensity $\tilde{\lambda}(t)$ is passed through a finite-time integrator (i.e., convolved with $h_\Delta(t)$). The frequency response $H_\Delta(f)$ of the finite-time integrator is given by:

$$H_\Delta(f) = \exp\{-j\pi f\Delta\} \cdot \Delta \cdot \sin(\pi f\Delta)/\pi f\Delta. \tag{26}$$

$H_\Delta(f)$ is a low-pass filter that attenuates the high frequency components in $\tilde{\lambda}(t)$. The attenuation depends upon the product of the bin width and the frequency of interest.

Second, the output of the finite-time integrator is then sampled at intervals equal to the bin width. If the integrator output is band-limited so that its highest frequency component is less than $1/2\Delta$, then all of the information contained in the convolution $\tilde{\lambda}(t) \otimes h_\Delta(t)$ is preserved in its samples. If components at frequencies larger than $1/2\Delta$ occur in the integrator output, they will be represented as low-frequency components in the sampled signal. This phenomenon is termed "aliasing" (Oppenheim and Schafer, 1975). Since $H_\Delta(f)$ is not band-limited (Eq. 26), $\tilde{\lambda}(t)$ must have no frequency larger than $1/2\Delta$ to prevent aliasing.

Consequently, the process of placing triggered pulses into bins is mathematically equivalent to a series of transformations on $\tilde{\lambda}(t)$ (Eq. 24). As expressed by these transformations, the accuracy of the representation of $\tilde{\lambda}(t)$ in the sequence $\{x_m\}$ depends upon the bin width $\Delta$. The bin width must be less than $1/2f_{\max}$ [$f_{\max}$ is the highest frequency component in $\tilde{\lambda}(t)$] to prevent aliasing. In general, the accuracy of the representation of $\tilde{\lambda}(t)$ by $\{x_m\}$ increases with smaller values of the bin width.

*Accumulation of the PST Histogram*

The contents of bins that occur at the same time relative to a set of stimulus markers are added together (or accumulated) to form the PST histogram. If the stimulus markers are periodic and occur every $M\Delta$, the contents of the $m^{\text{th}}$ bin of the PST histogram $g_m$ are given by:

$$g_m = \sum_{r=0}^{R-1} x_{m+rM}, \tag{27}$$

where the $x_{m+rM}$ denotes the contents of the $m^{\text{th}}$ bin after the $r^{\text{th}}$ stimulus marker and $R$ denotes the number of stimulus markers in the measurement interval. This computation is similar to the averaging of a periodic wave form from its samples (Braun, 1975). The computational procedure described by Eq. 27 can be interpreted as a linear,

shift-invariant digital filter (Oppenheim and Schafer, 1975) having input $\{x_m\}$ and output $\{g_m\}$ with unit sample response $\{h_m\}$. If no aliasing occurred in the time-quantization process, the frequency response of this digital filter is given by:

$$H_{\mathrm{PST}}(e^{j2\pi f\Delta}) = \exp\{j\pi fM(R-1)\Delta\}\cdot\sin(\pi fRM\Delta)/\sin(\pi fM\Delta) \qquad (28)$$

The magnitude of $H_{\mathrm{PST}}(e^{j2\pi f\Delta})/R$ is unity at integer multiples of the frequency $f = 1/M\Delta$.

*Summary of PST Histogram Computation*

By combining Eqs. 24 and 27, the expected value of a PST histogram is given by:

$$E[g_m] = h_m * [\tilde{\lambda}(t) \otimes h_\Delta(t)] \,|_{\,t=(m+1)\Delta}, \qquad (29)$$

where * denotes the convolution of sequences. Under certain circumstances, the relationship between $\tilde{\lambda}(t)$ and $E[g_m]$ is particularly simple. If $\tilde{\lambda}(t)$ contains frequency components only at the frequencies $k/M\Delta$, Eq. 29 is written:

$$E[g_m] = R\cdot[\tilde{\lambda}(t) \otimes h_\Delta(t)] \,|_{\,t=(m+1)\Delta}, \qquad (30)$$

so that:

$$[\tilde{\lambda}(t) \otimes h_\Delta(t)] \,|_{\,t=(m+1)\Delta} = E[g_m]/R. \qquad (31)$$

If the bin width is chosen small enough so that $\tilde{\lambda}(t)$ is approximately constant over the duration of a bin (i.e., $f_{\max} \ll 1/2\Delta$), the convolution in Eq. 31 can be approximated by $\tilde{\lambda}(m\Delta)\Delta$ so that:

$$\tilde{\lambda}(m\Delta) = E[g_m]/(R\cdot\Delta). \qquad (32)$$

Under these conditions, the expected value of a PST histogram is linearly related to the average intensity of the triggered pulse train evaluated every $\Delta$.

The relationship between $\lambda(t)$ and $\tilde{\lambda}(t)$ is given by Eq. 9. The effect of interfering signals is, generally speaking, to modify the high-frequency content of $\lambda(t)$. If $\lambda(t)$ does not contain components in the affected high-frequency regions, $\lambda(t)$ and $\tilde{\lambda}(t)$ are approximately equal. The ensemble average of the intensity of the spike train is then proportional to the expected value of the PST histogram and Eq. 32 becomes in this instance:

$$\lambda(m\Delta) = E[g_m]/(R\cdot\Delta). \qquad (33)$$

Under the assumptions given in this section, an unbiased estimate of $\lambda(t)$ at the times $m\Delta$ relative to the stimulus markers consists of dividing the amplitude of the PST histogram by the product of $R$, the number of stimulus markers, and $\Delta$, the bin width.

*An Application of the Model of PST Histogram Computation*

One example of applying the previous considerations is found in the analysis of auditory-nerve fiber responses to single tones. At low stimulus frequencies, PST histograms synchronized to each stimulus cycle indicate that the intensity of a single

fiber is "time-locked" to individual cycles of the stimulus (Kiang et al., 1965; Rose et al., 1967). At high frequencies, no such time locking is measured. There is no precise frequency separating the ranges over which these responses occur. Rather, the time-locking gradually diminishes for frequencies greater than 1 kHz; near 5–6 kHz, this time-locking is no longer measurable (Fig. 6). The question is whether this attenuation of time-locking in the 1–6 kHz frequency range could be due to limitations in the PST histogram computation.

The recordings analyzed by Johnson (1974) were recorded from single auditory nerve fibers with KCl-filled glass micropipettes. With these microelectrodes, the noise-to-signal ratios ($\gamma$) of the recordings were usually less than 0.05 and the rise time of the spikes ($t_r$) less than 200 $\mu$s. The effect of random interfering signals is to filter the intensity of the spike train. The bandwidth of this filter (Eq. 22 with $\gamma = 0.05$ and $t_r = 200$ $\mu$s) is 15.9 kHz. The attenuation of this filter is not sufficient to account for the measured decrease in the synchronized response obtained in the 1–6 kHz range (Fig. 6).

Time-quantization effects depend on the relation between the frequency of interest and the bin width $\Delta$ (Eq. 28). Assuming that no aliasing occurs in this quantization process, these effects act as a low-pass filter $H_\Delta(f)$ on the ensemble average of the intensity. For the attenuation of this filter to be less than 1%, the bin width must be such that $|H_\Delta(f)| > 0.99$. This requirement implies that there be at least 13 bins for each stimulus period. The data shown in Fig. 6 were obtained from PST histograms having from 33 bins (for measuring responses synchronized to 6 kHz) to 200 bins (1 kHz) per period. Consequently, the computed bound of 13 bins is easily satisfied; time-quantization effects cannot account for the decreasing trend in the data over the 1–6 kHz range. One concludes that the decrease in the synchronized response over the 1–6 kHz range cannot be explained by measurement errors.

## THE COMPUTATION OF INTERVAL HISTOGRAMS

An interval histogram contains the number of interspike intervals of a given length that occur in a recording. The three basic steps in the computation of an interval histogram are: (*a*) pulses are triggered from the recorded spike train, (*b*) the interval between successive pulses is measured, and (*c*) this measurement is quantized and the contents of the appropriate bin of the histogram are incremented (Perkel, et al., 1967; Glaser and Ruchkin, 1976; Sanderson and Kobler, 1976). In the following analysis, the average intensity $\lambda(t)$ is assumed to be a constant. This case is equivalent to assuming that the spike train can be described as a stationary point process. No restrictions are placed upon the statistics of interspike intervals.

### *Description of the Computational Procedures*

The measured interval $\tilde{\tau}$ between successive triggered pulses ($\tilde{\tau} = \tilde{t}_{k+1} - \tilde{t}_k$ where $\tilde{t}_k$ is the measured time of occurrence of the $k^{\text{th}}$ spike) is equal to the interval $\tau$ between the corresponding spikes plus $\tau_j$, the jitter in the measured interval induced by the interfering signal present in the recording.

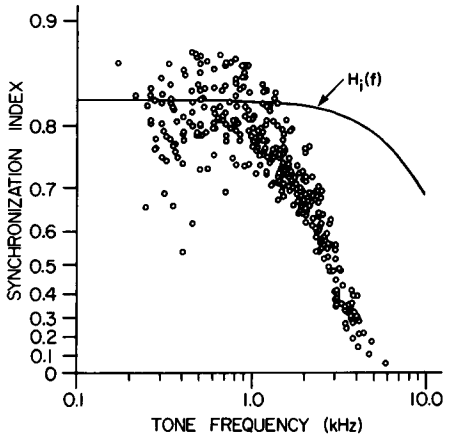


FIGURE 6

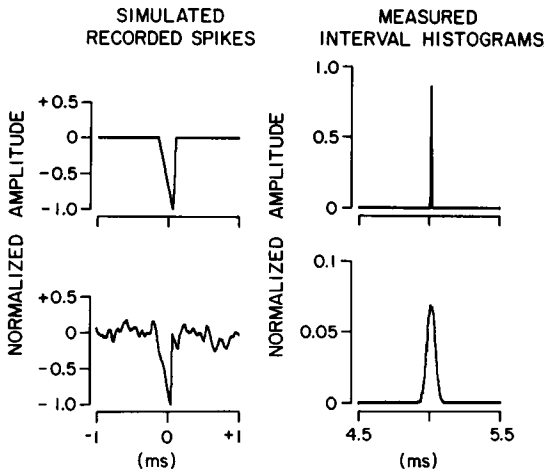


FIGURE 7

FIGURE 6 Evaluation of measurement limitations in computing the amplitude of stimulus-locked responses. PST histograms were computed from the responses of single auditory nerve fibers to single tones (Johnson, 1974). The duration of the histograms was equal to one cycle of the stimulus. The degree of time-locking of the responses to the stimulus was measured by computing the synchronization index $S_f$:

$$S_f = \frac{\sum_{m=0}^{M-1} g_m e^{-j(2\pi m/M)}}{\sum_{m=0}^{M-1} g_m}$$

The level of the tone was varied until the maximum value of $S_f$ was obtained. A total of 339 maxima from 233 auditory-nerve units are shown. The line denotes the frequency response $H_i(f)$ of the filter that models the effects of random interfering signals on measurements of $S_f$. The noise-to-signal ratio ($\gamma$) was assumed to be 0.05 and the spike time 200 $\mu$s. The magnitude of the frequency response was set equal to 0.83 for $f = 0$.

FIGURE 7 Effect of random interfering signals on measured interval histograms. Isolated simulated spikes are shown in the left column. The rise time of each spike was 200 $\mu$s. The right column contains the interval histograms computed from simulated spike trains. The vertical scale of each histogram was scaled by the number of spikes in the histogram (approximately 6,000). The bin width of each histogram was 5 $\mu$s. The simulated spike train was triggered from a 200-Hz sine wave. With no interfering noise (upper row), the resulting interval histogram contained a single dominant peak at an interval of 5 ms. With interfering noise (lower row with $\gamma = 0.1$ and bandwidth = 5 kHz), the interval histogram showed a spread of intervals about an average interval of 5 ms. The predicted standard deviation of this histogram (Eq. 37 with $R_i(\tau) = 0$) is 28.3 $\mu$s; the measured standard deviation of this histogram was 28.1 $\mu$s.

$$\tilde{\tau} = \tau + \tau_j. \tag{34}$$

From Eq. 6, this jitter is given by:

$$\tau_j = [i(\tilde{t}_k) - i(\tilde{t}_{k+1})]/m_s. \tag{35}$$

The jitter $\tau_j$ is assumed to be related to the characteristics of the interfering signal and to the spike wave form but not to the statistics of the underlying point process. Equivalently, $\tau_j$ is assumed to be statistically independent of $\tau$. The interfering signal $i(t)$ is assumed to be a stationary, Gaussian random process having zero mean, variance $\sigma^2$, and autocorrelation function $R_i(\tau)$. Therefore, $\tau_j$ is a Gaussian random variable having probability density function $h_j(\tau_j, \tilde{\tau})$ with zero mean and variance $\sigma_j^2$.

$$h_j(\tau_j, \tilde{\tau}) = (1/(2\pi\sigma_j^2)^{1/2}) \exp\{-\tfrac{1}{2}(\tau_j^2/\sigma_j^2)\}, \tag{36}$$

where $\sigma_j^2$ depends upon $\tilde{\tau}$ as follows:

$$\sigma_j^2 = 2[\sigma^2 - R_i(\tilde{\tau})]/m_s^2. \tag{37}$$

Let $p_\tau(\tau)$ be the probability density function (PDF) of $\tau$ and $p_{\tilde{\tau}}(\tilde{\tau})$ be the PDF of $\tilde{\tau}$. Since $\tilde{\tau}$ is the sum of the two independent random variables $\tau$ and $\tilde{\tau}_j$ (Eq. 34), $p_{\tilde{\tau}}(\tilde{\tau})$ is given by the convolution of $p_\tau(\tau)$ and $h_j(\tau_j, \tilde{\tau})$.

$$p_{\tilde{\tau}}(\tilde{\tau}) = \int_0^\infty p_\tau(\alpha) h_j(\tilde{\tau} - \alpha, \tilde{\tau}) \mathrm{d}\alpha. \tag{38}$$

Therefore, the presence of noise in the recording results in a smoothing of the interval distribution of the spike train by a Gaussian window (Fig. 7). The standard deviation $\sigma_j$ of the Gaussian window of the convolution varies with $\tilde{\tau}$; consequently, the smoothing of $p_\tau(\tau)$ varies with $\tilde{\tau}$. If the spectral characteristics of the noise are such that $R_i(\tau)$ is approximately zero for values of $\tilde{\tau}$ greater than $\tilde{\tau}_0$, then $\sigma_j$ equals $\sqrt{2}\gamma t_r$ for $\tilde{\tau} > \tilde{\tau}_0$. Since $|R_i(\tau)| < \sigma^2$, the maximum value of $\sigma_j$ (which corresponds to the maximum smoothing), is bounded by:

$$\max_{\tilde{\tau}} \sigma_j \leq 2\gamma t_r. \tag{39}$$

If the effective width of the Gaussian smoothing window is taken to be four times its standard deviation, the maximum width of the window is $8\gamma t_r$. If variations exist in $p_\tau(\tau)$ that are narrower than this maximum width, they may be smoothed. For example, discharge patterns that have nearly constant interspike intervals (e.g., recordings from pacemaker cells) have narrow interval probability density functions; the measurement of $p_\tau(\tau)$ for these patterns could well be affected by interfering background signals (Fig. 7).

The quantization of a measured interval $\tilde{\tau}$ to the duration of a bin is expressed by the function $\delta(m, \tilde{\tau}, \Delta)$ defined as:

$$\delta(m, \tilde{\tau}, \Delta) = \begin{cases} 1 & \text{if } m\Delta \leq \tilde{\tau} < (m + 1)\Delta, \\ 0 & \text{otherwise.} \end{cases} \tag{40}$$

The probability that $\delta(m, \tilde{\tau}, \Delta)$ equals 1 for given values of $\tilde{\tau}$ and $m$ is equal to the probability that $\tilde{\tau}$ lies in the interval $[m\Delta, (m + 1)\Delta)$.

$$\text{Prob}\,[\delta(m, \tilde{\tau}, \Delta) = 1] = \int_{m\Delta}^{(m+1)\Delta} p_{\tilde{\tau}}(\tilde{\tau})\mathrm{d}\tilde{\tau}. \tag{41}$$

As shown previously, this probability can be modeled as the sampled output of a finite-time integrator having $p_{\tilde{\tau}}(\tilde{\tau})$ as an input (Eqs. 29 and 30).

$$\text{Prob}\,[\delta(m, \tilde{\tau}, \Delta) = 1] = [p_{\tau}(\tilde{\tau}) \otimes h_{\Delta}(\tilde{\tau})]\,|_{\tilde{\tau}=(m+1)\Delta}. \tag{42}$$

The effects of the filtering and sampling processes defined in Eq. 41 are the same as those described for PST histograms.

Given the measured intervals $\tilde{\tau}_i$, $i = 1, \ldots N$, the contents of the $m^{\text{th}}$ bin of the interval histogram $I_m$ is computed by:

$$I_m = \sum_{i=1}^{N} \delta(m, \tilde{\tau}_i, \Delta). \tag{43}$$

Since the intervals are identically distributed, the expected value of $I_m$ is given by:

$$E[I_m] = N \cdot [p_{\tilde{\tau}}(\tilde{\tau}) \otimes h_{\Delta}(\tilde{\tau})]\,|_{\tilde{\tau}=(m+1)\Delta} \tag{44}$$

*Summary of Interval Histogram Computation*

The previous discussion presumed that the spike train can be described as a stationary point process. If the PDF of successive intervals $p_{\tau}(\tau)$ does not vary over values of comparable to $8\gamma t_r$, the effects of the interfering signal upon the measurement of the intervals obtained by triggering are small. In these cases, $p_{\tilde{\tau}}(\tilde{\tau})$ will be approximately equal to $p_{\tau}(\tau)$. The effects of interval quantization depend upon the relationship between the bin width and the frequency content of $p_{\tau}(\tau)$. If $\Delta$ is small enough so that the largest frequency in $p_{\tau}(\tau)$ is much less than $1/2\Delta$, then the interval quantization effects are small. If these conditions exist, the expected value of the interval histogram is proportional to samples of the interval probability density function $p_{\tau}(\tau)$.

$$p_{\tau}(m\Delta) = E[I_m]/(N \cdot \Delta). \tag{45}$$

Consequently, an interval histogram scaled by $(N\Delta)$ can serve as an unbiased estimate of the PDF of the intervals $\tau$.

*Application of the Model of Interval Histogram Computation*

Regular discharge patterns can be recorded from fibers in the vestibular nerve (Walsh et al., 1972). The measured interval histograms show a single dominant peak with some spread about the mean interval. The question is whether this spread is significant or whether it is due to measurement errors.

The effect of random interfering signals is to smooth the PDF of the intervals with a Gaussian-shaped window (Eq. 38). The spike trains analyzed by Walsh et al. (1972) were recorded with KCl-filled glass micropipettes. These recordings had signal-to-noise ratios ($\gamma$) less than 0.05 and spike rise times ($t_r$) less than 200 $\mu$s. With these values, the maximum window width ($8\gamma t_r$) is 0.08 ms. Interval histograms computed from regular-discharging spike trains have a spread of about 2 ms. Since the smoothing window is much narrower than the measured spread, the influence of random interfering noise on these data is not significant.

## DISCUSSION

The influence of each step in the computation of histograms on the overall accuracy of measurements of a recorded spike train's timing characteristics has been analyzed. For instance, random interfering signals do not greatly influence estimates of the average intensity of a spike train's intensity (e.g., Fig. 6). Such influences can be traced to the time-jitter term in Eq. 9. For reasonable values of noise-to-signal ratio ($\gamma$) and spike rise time ($t_r$), this jitter is small in comparison to time variations typically found in the intensity of a spike train. Deterministic interfering signals related to the stimulus tend to have a larger effect on estimates of the average intensity. This effect is related to the modulation term in Eq. 9; this term is proportional to the derivative of the interfering signal. Consequently, small, rapidly changing interfering signals can greatly affect estimates of the average intensity.

The exact values of $\gamma$ and $t_r$ obtained in a recording are functions of the neuron being recorded, the type of recording electrode, and the transfer function of the wave form amplification system. Electrolyte-filled glass micropipettes tend to isolate individual spikes well but have a limited bandwidth (3–8 kHz: Weiss et al., 1971). This limited bandwidth can reduce the rise-time of recorded spikes. Metal electrodes do not isolate spikes as well (i.e., larger values of $\gamma$ are encountered) but have a wider bandwidth. In an attempt to reduce $\gamma$, the recorded spike train can be filtered to reduce the energy of interfering signals in those regions of the spectrum where spikes do not contain energy. Such filtering can significantly reduce the amplitude of wide-band noise in a recording. Stimulus-related gross response in the recording very often has energy in the same spectral region as the spikes; consequently, attempts to remove such interfering signals by filtering may only serve to affect the spikes (i.e., increase $t_r$) as much as the unwanted interfering signal.

PST histograms display those components in the average of the intensity of a spike train which have frequencies harmonic with the stimulus marker frequency. Inharmonic components can be severely attenuated and thereby "washed out" of the histogram. This attenuation can be detrimental as well as beneficial. For instance, long-term variations in the statistics of a spike train (e.g., adaptational effects) will not be present in a PST histogram if higher-frequency response components are being measured. On the other hand, the attenuation of other response components can be intentional (e.g., analyzing the responses of single auditory-nerve fibers to multi-tone

stimuli) and can serve to simplify the task of analyzing a complicated response pattern. Intentional or not, the PST histogram may not display the entire response pattern and care should be taken in relating the histogram to the timing characteristics of the spike train.

PST and interval histograms have been related to the timing of discharges in a spike train. There are limitations to the accuracy of a histogram computed from stochastic spike trains because of the inherent variability of the histogram. This variability can, in principal, be reduced with larger amounts of data. However, each step in the computation of a PST or interval histogram also imposes a limitation on how accurately the histogram can be related to the characteristics of the spike train being studied. The accuracy of the representation of a spike train's average intensity is limited by the properties of the recorded spike train and the desired resolution (bin width) of the histogram. These limits do not depend on the finite number of spikes used in the computation of the histograms. Consequently, there are limits on the information that can be extracted from a recorded spike train with PST and interval histograms that cannot be improved by incorporating more data into the histograms.

## APPENDIX

The ensemble average $\tilde{\lambda}(t)$ of the pulse train triggered from a spike train recorded in the presence of an interfering signal $i(t)$ is given by Eq. 9. When $i(t)$ is a random process, $\tilde{\lambda}(t)$ is also a random process. The purpose of this appendix is to compute the expected value of $\tilde{\lambda}(t)$ when the spike train has a sinusoidal ensemble average (Eq. 14).

The ensemble average $\tilde{\lambda}(t)$ is given by Eq. 15. Expanding this equation, $E[\tilde{\lambda}(t)]$ is written

$$E[\tilde{\lambda}(t)] = \bar{\lambda} \cdot \left\{ 1 + 2S_f E\left[\cos 2\pi f\left(t + \frac{i(t)}{m_s}\right)\right] + \frac{1}{m_s} \cdot E[i'(t)] + \frac{2S_f}{m_s} E\left[i'(t) \cos 2\pi f\left(t + \frac{i(t)}{m_s}\right)\right]\right\}. \quad (46)$$

The interfering signal $i(t)$ is assumed to be a stationary Gaussian random process having zero mean, variance $\sigma^2$, and autocorrelation function $R_i(\tau)$. The second term on the right side of Eq. 46 is written

$$E\left[\cos 2\pi f\left(t + \frac{i(t)}{m_s}\right)\right] = \cos 2\pi f t \cdot E\left[\cos \frac{2\pi f i(t)}{m_s}\right] - \sin 2\pi f t \cdot E\left[\sin \frac{2\pi f i(t)}{m_s}\right]. \quad (47)$$

Since the PDF of $i(t)$ at any particular time $t$ is even, the expected value of an odd function of $i(t)$ is zero. Consequently, $E[\sin (2\pi f i(t)/m_s)]$ is zero. The remaining term is equivalent to the characteristic function of the PDF of $i(t)$.

$$E[\cos (2\pi f i(t)/m_s)] = \exp \{-\tfrac{1}{2}(2\pi f \sigma / m_s)^2\}. \quad (48)$$

Since $i(t)$ has zero mean, the third term in Eq. 46 is zero. Also, if the derivative of the correlation function $R_i(\tau)$ is defined at the origin, $i(t)$ and $i'(t)$ are independent random variables

(Middleton, 1960) and the fourth term in Eq. 46 is zero. Consequently, $E[\tilde{\lambda}(t)]$ does not depend upon the modulation term $i'(t)/m_s$ and is given by:

$$E[\tilde{\lambda}(t)] = \bar{\lambda} \cdot [1 + 2S_f \exp\{-\tfrac{1}{2}(2\pi f\sigma/m_s)^2\} \cos 2\pi ft]. \quad (49)$$

The figures were drawn by E.M. Marr, D.G. Beil, and J.D. Pusey and the manuscript typed by S.A. Nelson and D. Howe. Drafts of the manuscript were reviewed by Drs. N.Y.S. Kiang and W.T. Peake. The author benefited from many discussions with Dr. T.R. Bourk; Dr. Bourk also provided the spike train recordings illustrated in Figs. 1 and 2. Dr. T.F. Weiss not only reviewed many versions of the manuscript, but also provided many helpful criticisms and timely suggestions.

This work was supported by U.S. Public Health Service Grants 5 T01 GM01555, 5 R01 NS01344, 5 R01 NS11000, and 5 P01 GM14940.

*Received for publication 23 June 1977 and in revised form 20 February 1978.*

## REFERENCES

BRAUN, S. 1975. The extraction of periodic waveforms by time domain averaging. *Acustica.* **32**:69–77.

COX, D. R., and P. A. W. LEWIS. 1966. The statistical analysis of series of events. Methuen's Monographs in Applied Probability and Statistics, John Wiley & Sons, Inc., New York.

COX, D. R. 1962. Renewal process. Methuen's Monographs in Applied Probability and Statistics. John Wiley & Sons, Inc., New York.

GESTELAND, R. C., B. HOWLAND, J. Y. LETTVIN, and W. H. PITTS. 1959. Comments on microelectrodes. *Proc. IRE.* **47**:1856–1862.

GLASER, E., and D. J. RUCHKIN. 1976. Principles of Neurobiological Signal Analysis. Academic Press, Inc., New York. 291–371.

JOHNSON, D. H. 1974. The response of single auditory-nerve fibers in the cat to single tones: Synchrony and average discharge rate. Ph.D. Thesis, Department of Electrical Engineering, Massachusetts Institute of Technology, Cambridge, Mass.

PERKEL, D. H., G. L. GERSTEIN, and G. P. MOORE. 1967. Neuronal spike trains and stochastic point processes. I. The single spike train. *Biophys. J.* **7**:391–418.

KIANG, N. Y. S., T. WATANABE, E. C. THOMAS, and L. F. CLARK. 1965. Discharge Patterns of Single Fibers in the Cat's Auditory Nerve. MIT Research Monograph. The M.I.T. Press, Cambridge, Mass: 79–83.

MIDDLETON, D. 1960. An Introduction to Statistical Communication Theory, McGraw-Hill Book Company, Inc., New York: 374–375.

OPPENHEIM, A. V., and R. W. SCHAFER. 1975. Digital Signal Processing, Prentice-Hall, Inc., Englewood Cliffs, N.J.

ROSE, J. E., J. F. BRUGGE, D. J. ANDERSON, and J. E. HIND. 1967. Phase-locked response of low-frequency tones in single auditory nerve fibers of the squirrel monkey. *J. Neurophysiol.* **30**:769–793.

SANDERSON, A. C., and B. KOBLER. 1976. Sequential interval histogram analysis of non-stationary neuronal spike trains. *Biol. Cybern.* **22**:61–71.

SNYDER, D. L. 1975. Random Point Processes. John Wiley & Sons, New York.

WALSH, B. T., J. B. MILLER, R. R. GACEK, and N. Y. S. KIANG. 1972. Spontaneous activity in the eighth cranial nerve of the cat. *Int. J. Neurosci.* **3**:221–236.

WEISS, T. F., W. T. PEAKE, and H. S. SOHMER. 1971. Intracochlear potential recorded with micropipets. II. Responses in the cochlear scalaes to tones. *J. Acoust. Soc. Am.* **50**:587–601.